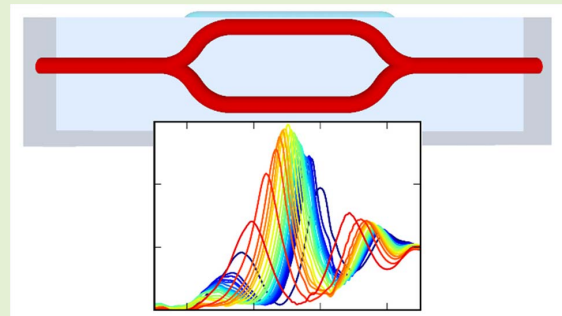


# Mach-Zehnder Interferometer-Based Evanescent Refractometer Inscribed at the Surface of Eagle2000 by Femtosecond Laser Writing

Vítor A. Amorim<sup>1</sup>, João M. Maia<sup>1</sup>, Duarte Viveiros<sup>1</sup>, and P. V. S. Marques<sup>1</sup>

**Abstract**—The potential of evanescent Mach-Zehnder interferometers, embedded in Eagle2000 substrates, as refractive index sensors was assessed. For that, femtosecond laser direct writing and wet etching were used to fabricate and expose the sensing arm at the surface of the glass substrate, while keeping the reference arm buried. From the analysis of the structures' spectral response, we found that the wavelength shift of the different order peaks increased greatly for refractive indices nearing that of the glass, indicating a greater overlap between the guided mode's evanescent field and the external medium. Therefore, a maximum sensitivity of 10271 nm/RIU was obtained at a refractive index of 1.491. The sensitivity in the refractive index range of water-based solutions was, on the other hand, limited to  $446 \pm 39$  nm/RIU. Due to the geometry of the device, applications with films deposited at the surface of the substrate and PDMS based microfluidic channels can be explored.



**Index Terms**—Femtosecond laser direct writing, integrated optical sensor, Mach-Zehnder interferometer, refractive index sensing.

## I. INTRODUCTION

THE use of Mach-Zehnder interferometers (MZI) produced with femtosecond laser fabrication techniques has been demonstrated in different application areas, namely in optical communications (in intensity modulators [1], [2], interleavers [3], and add-drop multiplexers [4]) and optical sensing. The later has seen progress in the quantification of

physical parameters such as temperature [5], [6], curvature [6]–[8], strain [5], relative humidity [9], pressure [10], [11] and refractive index [12], and biological parameters like glucose [13], bovine serum albumin [14], and E. Coli [15].

In recent years, the number of optical fiber based MZI sensors developed with femtosecond laser techniques has grown rapidly, with dozens of works having been published. Works developed in bulk substrates are, on the other hand, scarce, with only a handful of studies surfacing from our literature search, namely those reported by Crespi *et al.* [13] and Zhang *et al.* [16] for refractive index sensing, and a short mention of a temperature sensor by Lapointe *et al.* [17]. This is easily explained by, among other factors, the availability of optical fibers whose spectral characteristics are almost ideal, especially when compared to the challenges presented by the development of devices relying fully on the inscription of optical circuits using femtosecond laser writing. Furthermore, most of the sensing structures reported in the literature explore the use of MZIs where one of the arms intercepts the sensing medium, as opposed to relying on its evanescent interaction. This has obvious advantages over the interaction of the evanescent field, as the phase change is much larger, enabling higher sensitivities. Unfortunately, it requires drilling cavities,

Manuscript received July 3, 2020; revised August 29, 2020; accepted August 30, 2020. Date of publication September 3, 2020; date of current version December 16, 2020. This work was supported in part by the Fundação para a Ciência e a Tecnologia under Grant SFRH/BD/128795/2017 and in part by the Project “On Chip Whispering Gallery Mode Optical Microcavities For Emerging Microcontaminant Determination In Waters”—SAFE WATER, which is supported and co-funded by the European Commission, Directorate-General Communications Networks, Content and Technology (DG CONNECT) under the ERA-NET Cofund scheme—Horizon 2020 “Horizon 2020—the Framework Programme for Research and Innovation (2014-2020).” The associate editor coordinating the review of this article and approving it for publication was Prof. Marco Petrovich. (Corresponding author: Vítor A. Amorim.)

The authors are with the CAP—Centre for Applied Photonics, INESC TEC, 4150-179 Porto, Portugal, and also with the Department of Physics and Astronomy, Faculty of Sciences, University of Porto, 4169-007 Porto, Portugal (e-mail: vitor.a.amorim@inesctec.pt; joao.m.maia@inesctec.pt; carlos.d.viveiros@inesctec.pt; psmarque@fc.up.pt).

Digital Object Identifier 10.1109/JSEN.2020.3021586

which, in the case of optical fibers, increases its fragility. Also, and probably most importantly, geometries requiring the use of cavities hinder, or even prohibit, the use of standard lithographic techniques for the deposition of thin-films for the creation of more complex devices. By using an evanescent interaction scheme, it is possible to avoid such issues at the cost of sensitivity, with robust planar substrates facilitating the deposition process.

As such, in this work we report the refractive index sensing capabilities of MZIs inscribed in Eagle2000 substrates using femtosecond laser direct writing and wet etching. For that, the reference arm was buried in the substrate, while the sensing arm was manufactured at the surface of the substrate as to enable the interaction between the evanescent field of the guided mode and the external medium. The impact of the sensing arm's depth in the device's spectral response was studied from 700 to 1300 nm for refractive indices between 1.000 and 1.500. Finally, the wavelength shift and the respective sensitivity of the different fringe orders were evaluated as a function of the refractive index, and the results compared with the literature.

## II. EXPERIMENTAL PROCEDURE

In this work, a fiber amplified femtosecond laser (Satsuma HP, from Amplitude Systèmes)—running at 515 nm with a repetition rate of 1 MHz and a pulse duration of approximately 250 fs—was used to inscribe the MZIs in alkali-free borosilicate glass (Eagle2000) at a minimum depth of  $\approx 25 \mu\text{m}$ . A Workshop of Photonics workstation, equipped with Aerotech direct-drive stages (ANT130XY-110 PLUS and ANT130V-5 PLUS), was employed to scan the substrate orthogonal to the linearly polarized laser beam. The laser beam's polarization was adjusted to be parallel to the writing direction, with the scanning direction being maintained to avoid the Quill effect [18]. To drive non-linear absorption, the laser beam was focused inside the glass substrate using a 0.42 numerical aperture plan apochromat objective (Mitutoyo M Plan Apo NIR 50x). The laser beam's pulse energy and the stages' scan velocity were fixed at 125 nJ and 6 cm/s, respectively, as these parameters have produced good quality waveguides nearing the cut-off at longer wavelengths [19], [20], increasing the overlap between the guided mode and the external medium. The sensing arm was then translated to the surface through wet etching using an HF 1%/HCl 37% 10/2 (V/V) solution to avoid surface roughness [20]. Before characterization, the side facets of the substrate were also polished. This was done primarily to remove damage induced by the laser beam at the air/glass boundary and to eliminate the portion of waveguide that was etched at the facet due to etching selectivity. To characterize the MZIs', a broadband source was coupled to a single-mode fiber (SMF-28) which in turn was butt-coupled to the entrance facet of the fabricated structure. The light that propagates through the MZI is then retrieved by a second butt-coupled optical fiber at the exit facet. This was achieved in an Elliot Martock MDE881 stage with piezo controls (Dali E-2100), where the substrate and the input/output optical fibers were fixed. The retrieved light

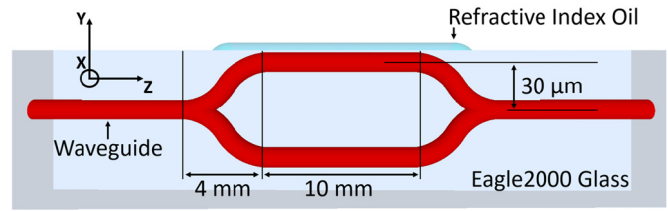


Fig. 1. Schematic of the MZIs fabricated and studied in this work.

was then guided to an optical spectrum analyzer (Yokogawa AQ6370D), where it was inspected from 700 nm to 1300 nm with a resolution of 2 nm. To isolate the spectral characteristics of the light source from that of the MZI, periodic normalizations were made to minimize the influence of small power fluctuations. Also, to minimize Fresnel reflections at the input/output fibers/facets, index matching (Cargille series: AA  $n_D^{25^\circ\text{C}} = 1.4580 \pm 0.0002$ ) was used.

## III. EXPERIMENTAL RESULTS AND DISCUSSION

In this study, several MZIs were fabricated in 24 mm long Eagle2000 substrates while varying their inscription depth in steps of  $0.5 \mu\text{m}$ . A schematic of the inscribed MZIs' structure is depicted in Fig. 1. As can be seen, of the total 24 mm, 18 mm were reserved to the MZI, while the remaining 6 mm were just straight waveguides to connect the structure to the substrate's facets. Furthermore, the geometrical path length of both MZI's arms is identical, with one of them being inscribed closer to the surface—enabling the interaction between the guided mode and the external medium—and the other buried  $60 \mu\text{m}$  below—acting as a reference. This was achieved with the implementation of 4 mm long vertical Y-junctions at the extremities of the arms, also enabling the interaction region to be limited to 10 mm. The cross-section of the optical waveguides used in the six MZIs studied in this work is depicted in Fig. 2, with the non-numbered cross-sectional image representing the buried optical waveguides fabricated by laser direct writing. The cross-section of the sensing arm is, on the other hand, numbered, and this numeration will be used throughout this work. Also, increasing numeration represents an increase in the MZI depth by  $0.5 \mu\text{m}$ . In the figure, one can see that the cross-section of the sensing arm was partially removed in order to enhance the amount of evanescent field interacting with the external medium. Since the sensing arm was brought to near the surface by wet-etching, the sample's surface was not completely flat after the process due to some residual etching anisotropy between exposed and non-exposed volumes.

As stated previously, the length of the MZI's arms is balanced. Therefore, assuming a single-mode behavior, the phase difference ( $\Delta\Phi$ ) attained by the guided mode interacting with the external medium in relation to the one confined to the glass substrate is described by:

$$\Delta\Phi(\lambda) = \frac{2\pi}{\lambda} L (n_{\text{buried}}(\lambda) - n_{\text{surface}}(\lambda)) \quad (1)$$

where  $\lambda$  is the vacuum wavelength,  $L$  is the interaction length of 10 mm defined for the structure, and  $n_{\text{buried}}(\lambda)$  and  $n_{\text{surface}}(\lambda)$  are the effective refractive index of the guided

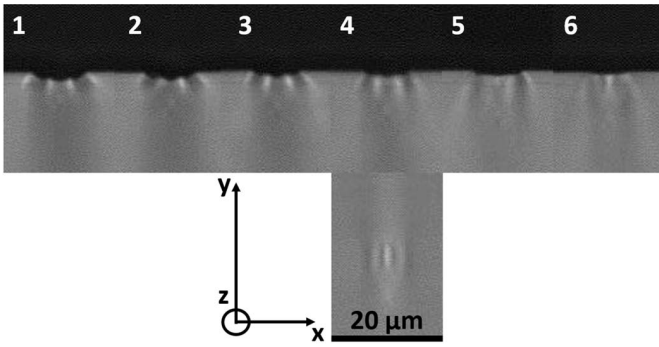


Fig. 2. Transmission mode optical microscope images of the cross-section of the MZIs' top arm (numbered), and the rest of its structure (not numbered). Inscription depth increases  $0.5 \mu\text{m}$  with increasing numeration. Laser inscription was made from the top to the bottom.

mode confined by the substrate and the one interacting with the external medium, respectively [16]. Theoretically, and assuming that the optical power in both MZI's arms is identical, the insertion loss (IL) induced by the MZIs should then be expressed as:

$$\text{IL}(\lambda) = -10\log_{10} \left( \frac{1}{2} [1 + \cos(\Delta\Phi(\lambda))] \right) \quad (2)$$

indicating that its spectral response is composed of periodical fringes. By using the condition for destructive interference— $\Delta\Phi = \pi(2m + 1)$ —and eq. (1), we can deduce that the location of the insertion loss peaks is defined as:

$$\lambda_m = \frac{2L(n_{\text{buried}}(\lambda) - n_{\text{surface}}(\lambda))}{2m + 1} \quad (3)$$

where  $m$  is the fringe order. If the effective refractive index of the mode travelling in the sensing arm is altered due to the external medium, the variation in the peak's wavelength can be expressed by:

$$|\Delta\lambda_m| = \frac{2L\Delta n_{\text{surface}}(\lambda)}{2m + 1} \quad (4)$$

where  $\Delta n_{\text{surface}}(\lambda)$  is the variation induced in the effective refractive index of the sensing arm's mode. On the other hand, if the dispersion is negligible, the free spectral range is given by:

$$\Delta\lambda_{FSR} \approx \frac{\lambda^2}{L(n_{\text{buried}}(\lambda) - n_{\text{surface}}(\lambda))} \quad (5)$$

Fig. 3 depicts the insertion loss spectra of the six different MZIs studied in this work for different Cargille refractive index oils between 1.000 and 1.480 ( $n_D^{25^\circ\text{C}}$ ). The spectra for  $n_D^{25^\circ\text{C}}$  equal to 1.490 and 1.500 were not plotted for clarity purposes. As expected from eq. (2), the insertion loss spectra present an interference fringe pattern. The fringe contrast is, however, seen to depend on the wavelength and the sensing arm depth, something that is not contemplated in eq. (2) due to the assumption that the optical power is always equal in both arms. First, the fringes appear to be confined to a wavelength window whose upper limit redshift as the depth of the sensing arm increases. And second, the fringe contrast is seen to grow for a larger depth of

the sensing arm. The cause of this behavior is most likely two-fold. 1) The spectral characteristics of near-surface optical waveguides are known to depend on its dimensions and depth (i.e. distance to the surface). In [20], we observed that the loss at longer wavelengths decreases sharply for a greater waveguide depth, meaning that the loss difference experienced by the sensing and reference arm is negligible, in the wavelength range of the present study, whenever the sensing arm's surface to core center separation is  $4 \mu\text{m}$  or greater. In this work, the deepest sensing arm has a surface to core center separation of roughly  $2 \mu\text{m}$ , explaining the increase in contrast and the redshift observed at the upper limit of the wavelength window. 2) A wavelength-dependent power imbalance in both arms created by unoptimized Y-junction splitters [21]. Another aspect that can be observed in Fig. 3 is the increase in free spectral range as the depth of the sensing arm and, consequently, its dimensions increase. From eq. (5), we can see that this derives from the term  $(n_{\text{buried}}(\lambda) - n_{\text{surface}}(\lambda))$ , as the presence of a larger portion of the original waveguide together with a smaller interaction between the guided mode and the external medium leads to a smaller effective refractive index difference between both the interferometer arms. At last, and most importantly, a blueshift in the peaks' position is observed when the refractive index increases. This is expected from eq. (3), since, for a given fringe order, the term  $(n_{\text{buried}}(\lambda) - n_{\text{surface}}(\lambda))$  approaches zero whenever there is an increase in  $n_{\text{surface}}(\lambda)$  due to a higher external medium's refractive index.

The wavelength shift observed in the insertion loss peaks is depicted in Fig. 4 (a) for MZI number 2 to number 5 and for the different fringe orders. MZI number 1 and 6 were excluded from this study due to their small ratio between fringe contrast and full width at half maximum. The refractive indices of the different oils used were corrected for dispersion at the wavelength of the insertion loss peaks. As can be seen, the blueshift observed in all the peaks is monotonic but not linear, increasing greatly for refractive indices closer to that of the substrate ( $n_D = 1.5068$ ). A similar behavior was observed by Zhang *et al.* in fused silica optical fibers [12]. This derives from a larger evanescent interaction due to a decrease in the refractive index contrast at the surface. Furthermore, the wavelength shift is larger for MZIs produced at slightly greater depths, also increasing for higher-order peaks within a given MZI. From eq. (3) and (5) we can, however, deduce that the fringe order is smaller for MZIs fabricated with the sensing arm at greater depths. Therefore, the effect of the fringe order on the wavelength shift is seemingly contradictory. In the case of MZIs produced at different depths and according to eq. (4), an increase in wavelength shift can be expected whenever the decrease in the denominator (controlled by the fringe order) is greater than that of the numerator (established by  $\Delta n_{\text{surface}}(\lambda)$ ). On the other hand, an increase in wavelength shift for higher-order peaks within the same device requires an increase in  $\Delta n_{\text{surface}}(\lambda)$ , as the wavelength decreases, in such a way that the increase in the numerator is larger than that of the denominator. Such behavior may occur due to an increase in V-number, improving the guided mode's

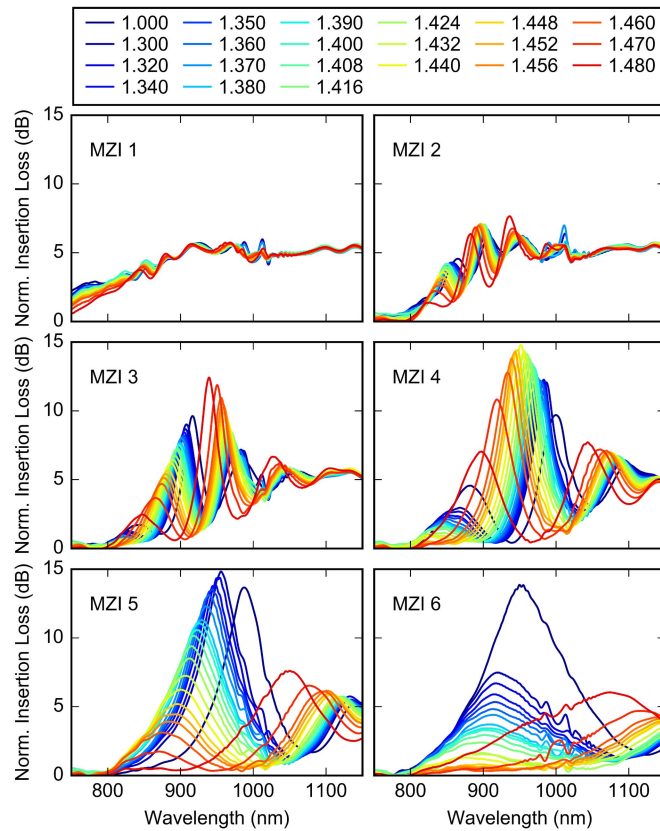


Fig. 3. Normalized insertion loss, as a function of wavelength, of Mach-Zehnder interferometers exposed to different Cargille refractive index oils at different sensing arm depths. The insertion loss spectra were normalized by subtracting the insertion loss of an embedded optical waveguide.

TABLE I

WAVELENGTH SENSITIVITY OF THE MACH-ZEHNDER INTERFEROMETERS TO REFRACTIVE INDEX FLUIDS IN THE RANGE OF WATER BASED SOLUTIONS

MZI	M <sup>TH</sup> ORDER	SENSITIVITY (NM/RIU)
2	$m_2$	$-51 \pm 10$
	$m_2+1$	$-51 \pm 16$
	$m_2+2$	$-82 \pm 17$
3	$m_3$	$-52 \pm 10$
	$m_3+1$	$-62 \pm 21$
	$m_3+2$	$-138 \pm 10$
4	$m_4$	$-93 \pm 20$
	$m_4+1$	$-252 \pm 24$
	$m_4+2$	$-255 \pm 16$
5	$m_5$	$-103 \pm 21$
	$m_5+1$	$-446 \pm 39$

confinement and bringing it closer to the surface, which in turn increases its overlap with the external medium and, therefore,  $\Delta n_{surface}(\lambda)$ .

Fig. 4 (b) displays the sensitivity of the different fringe orders plotted in Fig. 4 (a). As anticipated, the sensitivity is relatively small for refractive indices below 1.450, increas-

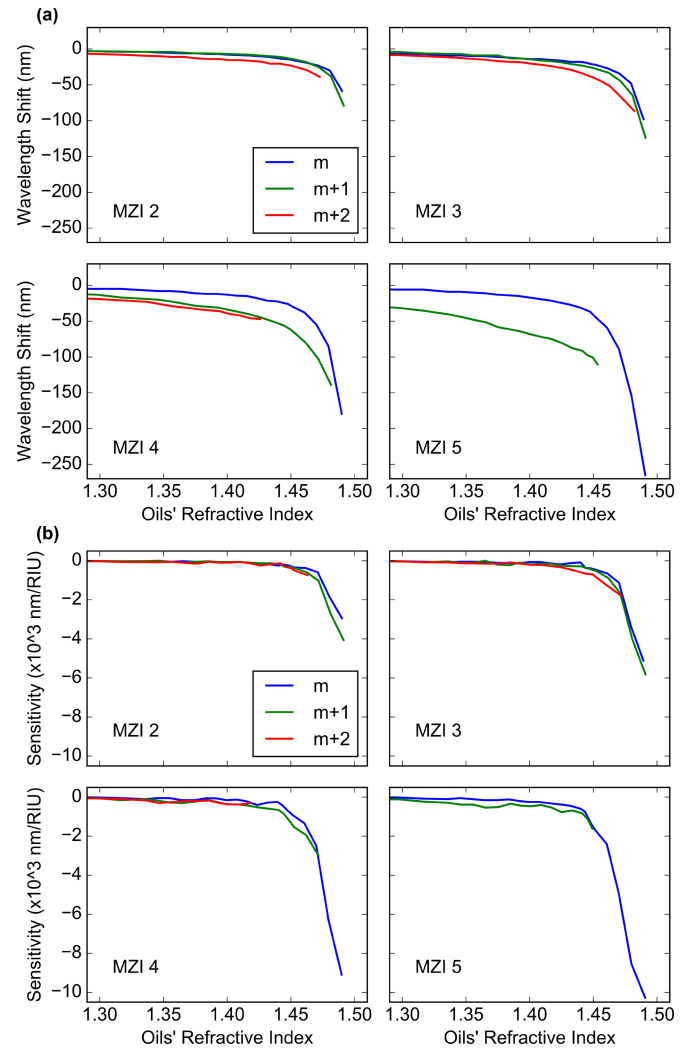


Fig. 4. Normalized wavelength shift (a) and sensitivity (b) of the different fringe orders, for MZI number 2 to 5, as a function of the external medium's refractive index.

ing rapidly for refractive indices above that. The maximum sensitivity was seen to increase for MZIs manufactured at greater depths, reaching  $\approx 10271$  nm/RIU at a refractive index of 1.491 for MZI number 5. For comparison, the device developed by Zhang *et al.* reached a peak sensitivity of  $\approx 3000$  nm/RIU at a refractive index of 1.432 [12].

A more interesting sensing region is the one in the range of water-based solutions, where the sensitivity is much lower but the applications more frequent. Therefore, the wavelength shift's study was also performed for refractive indices between  $\approx 1.336$  and  $1.376$ , as depicted in Fig. 5. Again, a larger sensing arm depth and a higher fringe order are seen to produce larger wavelength shifts. Although the wavelength response is not linear, it can be considered as such for a narrow refractive index range. Therefore, a linear fit was made to the results in fig. 5 in order to assess the average wavelength sensitivity in this range. The results are plotted in table I, summarizing what has been discussed above. In this study, a maximum sensitivity of  $-446 \pm 39$  nm/RIU was found for

TABLE II  
COMPARISON BETWEEN THE SENSITIVITY DISPLAYED BY DEVICES REPORTED IN THE LITERATURE AND IN THIS WORK

PLATFORM	INTERACTION METHOD	SENSITIVITY (NM/RIU)	REFRACTIVE INDEX RANGE	REFERENCES
Optical Fiber	Direct	≈10000 - 18000	≈1.30 - 1.36	[14, 15, 22-28]
Substrate	Direct	1500	≈1.33	[13]
Optical fiber	Evanescent	≈15 - 593	≈1.30 - 1.37	[29-33]
Substrate	Evanescent	122.4	≈1.33 - 1.38	[16]
Substrate	Evanescent	446±39	1.336 - 1.375	This work

This comparison was restricted to devices developed using femtosecond laser techniques and to a refractive index range compatible with water-based solutions.

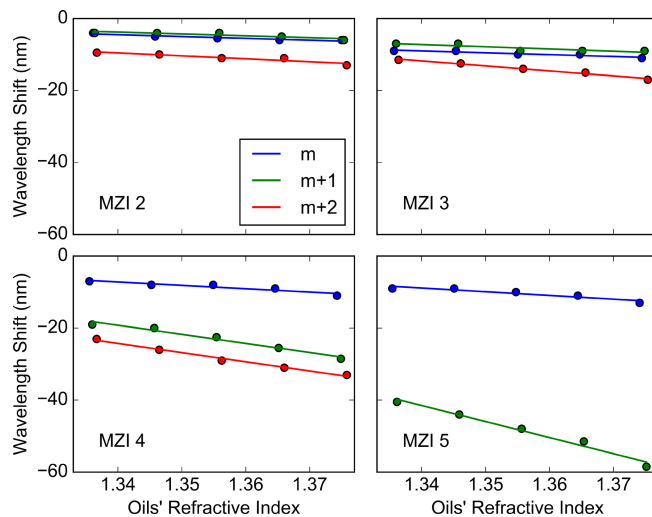


Fig. 5. Normalized wavelength shift of the different fringe orders, for MZI number 2 to 5, in the refractive index range of water-based solutions. Experimental data points were fitted to a linear equation.

refractive indices in the range of water-based solutions, making these devices interesting in specific applications.

Finally, a comparison between devices reported in the literature and the ones developed in this work can be found in table II for a refractive index range around water-based solutions. This comparison was limited to MZIs manufactured with femtosecond laser techniques, with both direct and evanescent interaction methods being considered. As can be observed, an obvious difference between devices using the evanescent and direct interaction methods exists, with the former yielding sensitivities in the range of the hundreds of nm/RIU while the later yields thousands to over ten thousand nm/RIU. This difference is fundamentally unavoidable. Among the few devices reported using evanescent interaction, however, our device demonstrated a good sensitivity, being only surpassed by the one developed by Liao *et al.* in an optical fiber [33]. The sensitivity can be further enhanced by the use of dielectric thin films such as TiO<sub>2</sub> [34].

#### IV. CONCLUSION

In this work, we demonstrated that Mach-Zehnder interferometers produced with one of its arms at the surface of Eagle2000 substrates can be used as refractometers. The arms'

physical path length was balanced, with the phase difference deriving solely from the interaction between the guided mode's evanescent field and the external medium. Therefore, a variation in the free spectral range was observed for different sensing arm depths. A lower loss in the sensing arm—achieved at greater depths—also meant that the fringe contrast could reach values of up to 15 dB. Unfortunately, wavelength-dependent power imbalance limited the contrast to a wavelength window of roughly 400 nm. Furthermore, wavelength sensitivity was seen to increase with the external medium's refractive index, growing dramatically for a refractive index close to that of the glass. Consequently, a maximum sensitivity of 10271 nm/RIU, at a refractive index of 1.491, was obtained. The sensitivity in the refractive index range of water-based solutions was limited to 446 ± 39 nm/RIU.

#### REFERENCES

- [1] G. Li, K. A. Winick, A. A. Said, M. Dugan, and P. Bado, "Waveguide electro-optic modulator in fused silica fabricated by femtosecond laser direct writing and thermal poling," *Opt. Lett.*, vol. 31, no. 6, pp. 739–741, Mar. 2006.
- [2] D. A. Presti, V. Guarepi, F. Videla, A. Fasciszewski, and G. A. Torchia, "Intensity modulator fabricated in LiNbO<sub>3</sub> by femtosecond laser writing," *Opt. Lasers Eng.*, vol. 111, pp. 222–226, Dec. 2018.
- [3] J. C. Ng, C. Li, P. R. Herman, and L. Qian, "Femtosecond laser writing of a flat-top interleaver via cascaded Mach-Zehnder interferometers," *Opt. Express*, vol. 20, no. 16, pp. 17894–17903, Jul. 2012.
- [4] V. A. Amorim, J. M. Maia, D. Alexandre, and P. V. S. Marques, "Monolithic add-drop multiplexers in fused silica fabricated by femtosecond laser direct writing," *J. Lightw. Technol.*, vol. 35, no. 17, pp. 3615–3621, Sep. 1, 2017.
- [5] W. W. Li, W. P. Chen, D. N. Wang, Z. K. Wang, and B. Xu, "Fiber inline Mach-Zehnder interferometer based on femtosecond laser inscribed waveguides," *Opt. Lett.*, vol. 42, no. 21, pp. 4438–4441, Nov. 2017.
- [6] W. W. Li and D. N. Wang, "Femtosecond laser inscribed straight waveguide in no-core fiber for in-line Mach-Zehnder interferometer construction," *Opt. Lett.*, vol. 43, no. 14, pp. 3405–3408, Jul. 2018.
- [7] P. Chen, X. Shu, and K. Sugden, "Compact assembly-free vector bend sensor based on all-in-fiber-core Mach-Zehnder interferometer," *Opt. Lett.*, vol. 43, no. 3, pp. 531–534, Feb. 2018.
- [8] D. P. Aldeiturriaga, L. R. Cobo, A. Quintela, and J. M. L. Higuera, "Curvature sensor based on in-fiber Mach-Zehnder interferometer inscribed with femtosecond laser," *J. Lightw. Technol.*, vol. 35, no. 21, pp. 4624–4628, Nov. 1, 2017.
- [9] G. Fu, L.-L. Ma, F.-F. Su, and M. Shi, "U-shaped micro-groove fiber based on femtosecond laser processing for humidity sensing," *Optoelectron. Lett.*, vol. 14, no. 3, pp. 212–215, May 2018.
- [10] Y. Liu, H. Lin, Y. Dai, A. Zhou, and L. Yuan, "Fiber in-line Mach-Zehnder interferometer for gas pressure sensing," *IEEE Sensors J.*, vol. 18, no. 19, pp. 8012–8016, Oct. 2018.

- [11] Y. Wang, Y. Liu, R. Gao, K. Cao, and S. Qu, "Mach-Zehnder interferometer based on a cross-type microchannel in SMS fiber structure for gas pressure sensing with high sensitivity," *Opt. Eng.*, vol. 57, no. 9, Sep. 2018, Art. no. 096101.
- [12] Y. Zhang, C. Lin, C. Liao, K. Yang, Z. Li, and Y. Wang, "Femtosecond laser-inscribed fiber interface Mach-Zehnder interferometer for temperature-insensitive refractive index measurement," *Opt. Lett.*, vol. 43, no. 18, pp. 4421–4424, Sep. 2018.
- [13] A. Crespi *et al.*, "Three-dimensional Mach-Zehnder interferometer in a microfluidic chip for spatially-resolved label free detection," *Lab Chip*, vol. 10, no. 9, pp. 1167–1173, Apr. 2010.
- [14] Z. Li *et al.*, "Label-free detection of bovine albumin based on an in-fiber Mach-Zehnder interferometric biosensor," *Opt. Express*, vol. 25, no. 15, pp. 17105–17113, Jul. 2017.
- [15] M. Janik, M. Koba, A. Celebańska, W. J. Bock, and M. Āsmietana, "Live E. Coli bacteria label-free sensing using a microcavity in-line Mach-Zehnder interferometer," *Sci. Rep.*, vol. 8, no. 1, Nov. 2018, Art. no. 17176.
- [16] D. Zhang, L. Men, and Q. Chen, "Femtosecond laser microfabricated optofluidic Mach-Zehnder interferometer for refractive index sensing," *IEEE J. Quantum Electron.*, vol. 54, no. 6, Dec. 2018, Art. no. 7600107.
- [17] J. Lapointe, M. Gagné, M. J. Li, and R. Kashyap, "Making smart phones smarter with photonics," *Opt. Express*, vol. 22, no. 13, pp. 15473–15483, Jun. 2014.
- [18] P. G. Kazansky *et al.*, "Quill writing with ultrashort light pulses in transparent materials," *Appl. Phys. Lett.*, vol. 90, no. 15, Apr. 2007, Art. no. 151120.
- [19] V. A. Amorim, D. Viveiros, J. M. Maia, and P. V. S. Marques, "Mass producible low-loss broadband optical waveguides in Eagle2000 by femtosecond laser writing," *IEEE Photon. Technol. Lett.*, vol. 31, no. 20, pp. 1658–1661, Oct. 15, 2019.
- [20] V. A. Amorim, J. M. Maia, D. Viveiros, and P. V. S. Marques, "Inscription of surface waveguides in glass by femtosecond laser writing for enhanced evanescent wave overlap," *J. Opt.*, vol. 22, no. 8, Aug. 2020, Art. no. 085801, doi: [10.1088/2040-8986/aba03f](https://doi.org/10.1088/2040-8986/aba03f).
- [21] V. A. Amorim, J. M. Maia, D. Alexandre, and P. V. S. Marques, "Optimization of broadband Y-junction splitters in fused silica by femtosecond laser writing," *IEEE Photon. Technol. Lett.*, vol. 29, no. 7, pp. 619–622, Apr. 1, 2017.
- [22] Y. Liu, G. Wu, R. Gao, and S. Qu, "High-quality Mach-Zehnder interferometer based on a microcavity in single-multi-single mode fiber structure for refractive index sensing," *Appl. Opt.*, vol. 56, no. 4, pp. 847–853, Feb. 2017.
- [23] Z. Li *et al.*, "Ultrasensitive refractive index sensor based on a Mach-Zehnder interferometer created in twin-core fiber," *Opt. Lett.*, vol. 39, no. 17, pp. 4982–4985, Sep. 2014.
- [24] L. Jiang, L. Zhao, S. Wang, J. Yang, and H. Xiao, "Femtosecond laser fabricated all-optical fiber sensors with ultrahigh refractive index sensitivity: Modeling and experiment," *Opt. Express*, vol. 19, no. 18, pp. 17591–17598, Aug. 2011.
- [25] M. Smietana, M. Janik, M. Koba, and W. J. Bock, "Transition between bulk and surface refractive index sensitivity of micro-cavity in-line Mach-Zehnder interferometer induced by thin film deposition," *Opt. Express*, vol. 25, no. 21, pp. 26118–26123, Oct. 2017.
- [26] M. Janik, A. K. Mysliwiec, M. Koba, A. Celebanska, W. J. Bock, and M. Smietana, "Sensitivity pattern of femtosecond laser micromachined and plasma-processed in-fiber Mach-Zehnder interferometers, as applied to small-scale refractive index sensing," *IEEE Sensors J.*, vol. 17, no. 11, pp. 3316–3322, Jun. 2017.
- [27] Y. Liu, M. Li, H. Sun, Y. Li, and S. Qu, "Ultrasensitive liquid refractometer based on a Mach-Zehnder micro-cavity in optical fibre fabricated by femtosecond laser-induced water breakdown," *J. Mod. Opt.*, vol. 63, no. 21, pp. 2285–2290, Jul. 2016.
- [28] X.-R. Dong *et al.*, "Microcavity Mach-Zehnder interferometer sensors for refractive index sensing," *IEEE Photon. Technol. Lett.*, vol. 28, no. 20, pp. 2285–2288, Oct. 2016.
- [29] P. Lu and Q. Chen, "Femtosecond laser microfabricated fiber Mach-Zehnder interferometer for sensing applications," *Opt. Lett.*, vol. 36, no. 2, pp. 268–270, Jan. 2011.
- [30] H. Zhang *et al.*, "A Mach-Zehnder interferometer based on a no-core fiber with in-fiber waveguides," *IEEE Photon. Technol. Lett.*, vol. 31, no. 13, pp. 1084–1087, Jul. 2019.
- [31] B. Li, L. Jiang, S. Wang, L. Zhou, H. Xiao, and H. Tsai, "Ultra-abrupt tapered fiber Mach-Zehnder interferometer sensors," *Sensors*, vol. 11, no. 6, pp. 2739–2729, Dec. 2011.
- [32] W. W. Li, D. N. Wang, Z. K. Wang, and B. Xu, "Fiber in-line Mach-Zehnder interferometer based on a pair of short sections of waveguide," *Opt. Express*, vol. 26, no. 9, pp. 11496–11502, Apr. 2018.
- [33] C. Liao, F. Zhu, P. Zhou, and Y. Wang, "Fiber taper-based mach-Zehnder interferometer for ethanol concentration measurement," *Micromachines*, vol. 10, no. 11, p. 741, Oct. 2019.
- [34] H. C. A. S. G. Vasconcelos, J. M. M. D. Almeida, C. M. T. Saraiva, P. A. D. S. Jorge, and L. C. C. Coelho, "Mach-Zehnder interferometers based on long period fiber grating coated with titanium dioxide for refractive index sensing," *J. Lightw. Technol.*, vol. 37, no. 18, pp. 4584–4589, Sep. 15, 2019.

**Vítor A. Amorim** received the B.Sc. degree in technological physics and the M.Sc. degree in physical engineering from the University of Porto, where he is currently pursuing the Ph.D. degree in physics. He joined the Centre for Applied Photonics, INESC TEC, in 2015, where he is currently enrolled in research activity. His current research interests include integrated optical devices fabricated by femtosecond laser direct writing for sensing applications.

**João M. Maia** received the B.Sc. degree in technological physics and the M.Sc. degree in physics engineering from the Faculty of Sciences, University of Porto, Portugal, in 2014 and 2016, respectively, where he is currently pursuing the Ph.D. degree in physics. In 2015, he joined the Centre for Applied Photonics (CAP), INESC TEC, Porto, Portugal, where he is doing research on femtosecond laser micromachining. His current research interests cover fabrication of optofluidic devices for chemical sensing and photopolymerization.

**Duarte Viveiros** received the degree in electronics and telecommunications engineering and the M.Sc. degree in energy networks and telecommunications engineering from the University of Madeira, Madeira, Portugal, in 2011 and 2013, respectively. He is currently pursuing the Ph.D. degree in physics with the Faculty of Sciences, University of Porto, Portugal, with the focus on the optical fiber sensors fabricated by femtosecond laser direct writing in collaboration with the Centre for Applied Photonics (CAP), INESC TEC, Porto, Portugal. His current research interests include optical sensors, femtosecond laser direct writing techniques for optical fiber and integrated optics, Bragg gratings, and long period gratings. He is a member of the University of Porto SPIE Student Chapter, SPIE—International Society for Optics and Photonics.

**P. V. S. Marques** is an Associate Professor with the Physics and Astronomy Department, Faculty of Sciences, Porto University, Portugal, and since October 2009, he is the Coordinator of the Center of Applied Photonics, INESC TEC and also the Director of the Micro and Nanofabrication Center, Porto University (CEMUP MNTEC). His current research interests include optical sensors, femtosecond laser direct writing techniques for integrated optics and microfabrication in general, microfluidics, Bragg gratings and active devices. He has published four world patents (patent family of 32), more than 100 scientific papers in international magazines and conferences and three book chapters.